1 Introduction

Although data on echinoderm biomineralization mostly come from studies on echinoids, it is widely accepted that all echinoderm classes build their skeletons using the same method of biomineralization, as inferred from very similar structures, properties, morphogenesis and organic molecules involved in the skeletogenesis (Dubois and Chen, 1989). Echinoderm skeletons are formed within the syncytium (i.e., a multinucleate cell) through a biologically controlled intracellular biomineralization process (e.g., Okazaki, 1960; Märkel 1986; Weiner and Addadi, 2011). They are composed of many calcite plates with a unique trabecular microstructure called stereom: herein lies the major synapomorphy of Echinodermata (e.g., Bottjer et al., 2006). In this Element, I summarize current and state-of-the-art knowledge of echinoderm biomineralization, with particular attention to the stereom microstructure and its functions. I also discuss methods for investigating stereom in fossil echinoderms, and highlight through case studies the great potential of micromorphological observations in determining the paleoanatomy and paleoecology of extinct groups of echinoderms.

2 Biomineralization, Structure and Biogeochemistry of the Echinoderm Skeleton

Larval and postmetamorphic skeletons of echinoderms are of both internal and mesodermal origin. However, they can be exposed to the external environment if the syncytial membranes are degraded (e.g., Märkel, 1986). The larval skeleton is composed of spicules made of a few rods that are almost completely resorbed at the end of the larval stage. The postmetamorphic skeleton, in turn, consists of numerous ossicles bound together by connective and/or muscle tissues that begin to form *de novo* just before settlement and metamorphosis (Hyman, 1955).

Sclerocytes (the so-called skeleton-forming cells, SFCs) along with odontoblasts (which are involved in the tooth formation) have long been considered the only cell types directly involved in biomineralization (Ameye, 1999). However, it has been recently shown that even nonspecialized epithelial cells may also be involved in this process (Vidavsky et al., 2014). Additionally, the role of phagocytes and/or spherulocytes in biomineralization has been recently hypothesized (Kołbuk et al., 2019). The formation of the skeleton takes place within vacuoles or vesicles that are typically enclosed in a syncytial pseudopodium formed by SFCs. Initially, the skeleton is being formed intracellularly and then extracellularly. Several ion transport systems, including special ion pumps, channels, exchargers and cotransporters, have been suggested to play a key role

in echinoderm biomineralization (for a review, see Dubois and Chen, 1989). It has been also suggested that organic components may be involved in this transport (Beniash et al., 1999; Wilt, 1999). Furthermore, as recently shown by Vidavsky et al. (2016), seawater with its ions can be directly incorporated into the cells of echinoid embryos by endocytosis. However, the exact pathway of ion transport into the calcification site in adult echinoderms is still uncertain. A generalized crystallization pathway in echinoderms has been proposed by Weiner and Addadi (2011; see also Figure 1A). According to this model, once ions have been transported to the vesicles, formation of the first disordered mineral phase (amorphous calcium carbonate ACC) initiates. Subsequently, the vesicles bearing ACC nanoparticles with occluded biomolecules are transported into the syncytium where translocation and secondary crystallization of nanograins (from disordered into a more ordered phase) proceeds on the organic template (for more details, see Weiner and Addadi, 2011; Seto et al., 2012).

The mature skeleton of echinoderms is composed of magnesian calcite comprising small amounts (up to about ~10 wt%) of stable amorphous calcium carbonate (ACC), water (< 0.2 wt%), and up to about ~1.6 wt% of intrastereomic organic matrix (Alberic et al., 2019). $MgCO_3$ content may vary widely from about 3 to 43.5 mole% (e.g., Schroeder et al., 1969). Skeletal Mg/Ca ratio in echinoderms can be affected by a number of environmental and physiological factors (such as ambient seawater Mg^{2+}/Ca^{2+} ratio, temperature, salinity, diet and "vital effects"; for a review, see Kołbuk et al., 2019; Kołbuk et al., 2020).

Under X-ray diffraction and polarizing microscopy, any individual ossicle behaves as a single calcite crystal (e.g., Donnay and Pawson, 1969; Yang et al., 2011). However, the crystal texture (i.e., coherence length [the average distance between imperfections in specific crystallographic directions] = 50–250 nm, and angular spread of perfect domains [degree of misalignment between perfectly coherent domains] = 0.1º) differs significantly from those observed in abiotic calcite (usually 500–800 nm and 0.01º, respectively). Furthermore, the crystal texture may differ among the different fabrics of the stereom in the same ossicle (Berman et al., 1993; Aizenberg et al., 1997). For instance, it has been shown that the perfect domains are more isotropic in the trabeculae of the open, regular stereom than in the lateral septa composed of imperforate stereom layers where coherence length is lower in the direction perpendicular to the *c*-axis (Aizenberg et al., 1997). Additionally, when broken, the echinoderm skeleton displays conchoidal fracture that reduces the brittleness of the material by dissipating strain energy and deflecting crack propagation (Berman et al., 1988). This unique property of stereom, that is generally harder, stiffer and stronger than inorganic calcite, has been ascribed to the involvement of organic molecules (the so-called intrastereomic organic matrix; IOM) in the

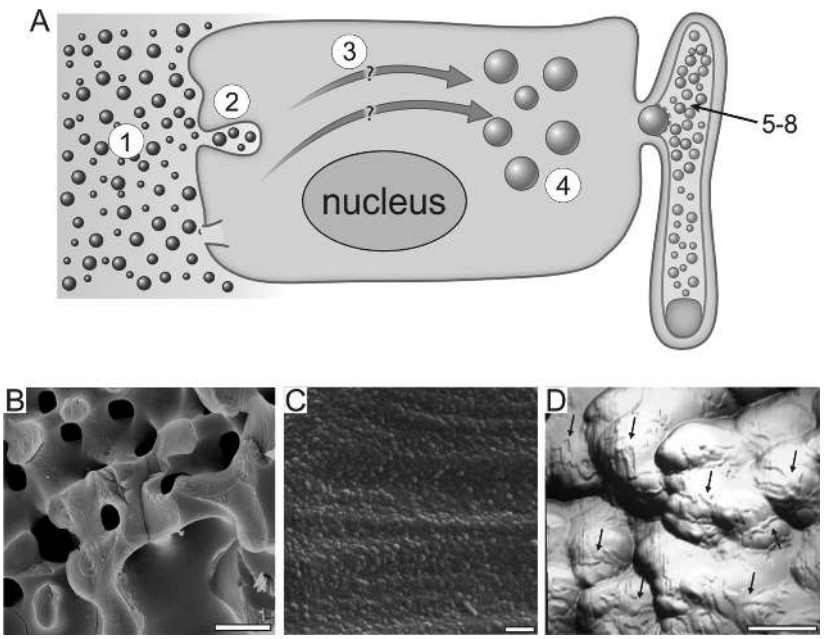

Figure 1 Biomineralization in echinoderms. A. Biomineralization pathway (redrawn and slightly modified after Weiner and Addadi, 2011): (1) the medium (seawater and/or body fluid) from which the ions are derived, (2) the ion-sequestering via endocytosis of seawater droplets and/or ion channels and/or transporters, (3) transport within the cell to vesicles, (4) vesicles in which the first disordered ACC phase forms, (5–8) transport of the ACC-bearing vesicles into the syncytium, translocation of the disordered ACC phase to the crystallization front and its transformation into more ordered phase. B. Fully mature mineralized tissue showing a concentric lamination revealed by slight acid etching (FESEM [Field Emission Scanning Electron Microscopy] micrograph). C. Magnification of the fractured stereom bar revealing nanogranular structure (FESEM micrograph). D. Magnification of the fractured stereom bar revealing nanograins with possible organic envelopes (arrows) (3D visualization of the height mode AFM [Atomic Force Microscopy] image). Scale bars: 10 µm (B), 200 nm (C), 100 nm (D), respectively.

biomineralization and their incorporation into the skeleton at different structural levels (e.g., Weiner, 1985). These organic components include various proteins and glycoproteins (N-glycoproteins, O-glycoproteins and terminal sialic acids), distribution of which may be variable, that is, N-glycoproteins are preferentially located in the putative amorphous subregions of the stereom whereas O-glycoproteins are localized in the subregion where skeletal growth is

inhibited (Ameye et al., 1998; Ameye et al., 2001). In general, IOM plays a significant role in the biomineralization of echinoderms by regulating the onset, orientation and growth rate of crystal formation, controlling the Mg content and stabilizing ACC.

The organic components are typically structured with the mineral phase within individual stereom trabeculae in a form of alternate and thin concentric layers (e.g., Dubois, 1991; Ameye et al., 1998; Figure 1B). These layers, at the nanoscale, reveal a nanocomposite structure: mineral grains, commonly 20–100 nm in diameter, are closely associated with an organic material (e.g., Oaki and Imai, 2006; Cuif et al., 2011; Seto et al., 2012; Figure 1C, D).

At the microscale, each ossicle appears in the form of a tridimensional fenestrated meshwork of trabeculae, the so-called stereom. Extensive studies on the skeletal microstructure have documented different stereom microfabrics that have similar morphogenesis (Dubois and Jangoux, 1990; Gorzelak et al., 2011; Gorzelak et al., 2014a; Figure 2). Initially stereom trabecular bars grow in

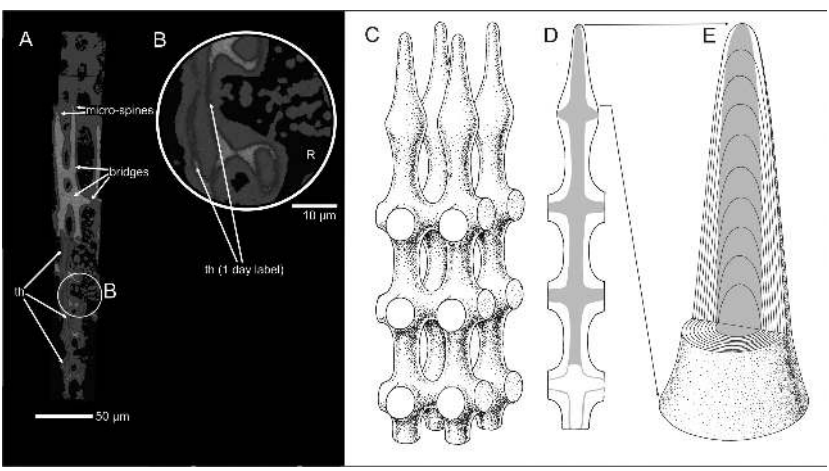

Figure 2 Stereom morphogenesis (compiled from Gorzelak et al., 2011). A. NanoSIMS maps of the $^{26}Mg/^{44}Ca$ distribution in labeled spine stereom of *Paracetrotus lividus* Lamarck during 1-day ^{26}Mg labeling event. B. Enlargements of the stereom showing 1-day thickening process ("th" and arrows) during the ^{26}Mg labeling event on the previously formed stereom bars. R = resin filled pores, blue regions = growth in normal (i.e., unlabeled) artificial seawater with normal $^{26}Mg/^{44}Ca$ ratio, red-yellow regions = enhanced $^{26}Mg/^{44}Ca$ ratio due to ^{26}Mg labeling. C–E. Model of stereom formation. Orange regions = distribution of ^{26}Mg label as observed in experiment, thin labeled thickening layer (bottom in D) is continuous with massive labeling.

a form of thin conical micro-spines. The neighboring micro-spines then fuse together by lateral bridges forming a thin meshwork of inner stereom that thickens simultaneously and very slowly by addition of thickening layers (Figure 2). The stereom pores may be eventually filled by secondary calcite to form perforate or imperforate stereom layers (Gorzelak et al., 2017a).

3 Stereom Types and Relationship to Phylogeny, Growth Rate and Investing Soft Tissues

Early work on skeletal microstructure in echinoderms recognized two basic types of stereom: regular (termed alpha) and irregularly arranged meshwork (termed beta) (Roux, 1970). Subsequently, however, Macurda and Meyer (1975) found that the stereom design in modern crinoids may be much more complex. The latter authors stressed that stereom may be quantified and introduced a new terminology for alpha and beta stereoms, which were then referred to as galleried and labyrinthic stereoms, respectively. In his seminal paper on echinoid microstructure, Smith (1980a) identified a variety of different stereom types, and provided their formal definitions (see Sections 3.1–3.8). This author pointed out that the stereom coarseness can be quantified using maximum pore diameter and trabecular thickness (measured in the narrowest point between adjacent pores) (Figure 3). He also stressed that the stereom microstructure can be controlled by three major factors: phylogeny, growth rate and type of investing soft tissue.

Phylogenetic signal in plate microstructure of echinoids was already noted by Nissen (1969) who pointed out that cidaroids in general display much more regular stereom in plates than any other groups of echinoids. Notable differences in the basic pattern of stereom design in plates and spines between different echinoid taxa were recognized by Smith (1980a, 1984, 1990) and Kroh and Smith (2010). Phylogenetic significance of stereom architecture in crinoids has also been emphasized by Simms (2011), who highlighted that the stereom design of columnal latera more likely reflects phylogeny than function. Simms argued that labyrinthic stereom is taxonomically widespread and plesiomorphic, whereas perforate stereom is apomorphic for Isocrinida.

Stereom appearance may be also affected by the rate of calcification. For instance, Pearse and Pearse (1975) found that well-fed and fast-growing echinoids produced their plates dominated by opaque growth zones (composed of regular stereom), whereas starving and slow-growing individuals formed plates composed of translucent zones (having more irregular stereom). Additionally, Smith (1980a) noted that trabecular thickness and porosity may be influenced by growth rate. He argued that rapid growth is commonly associated with open stereom, whereas reduced growth rate is

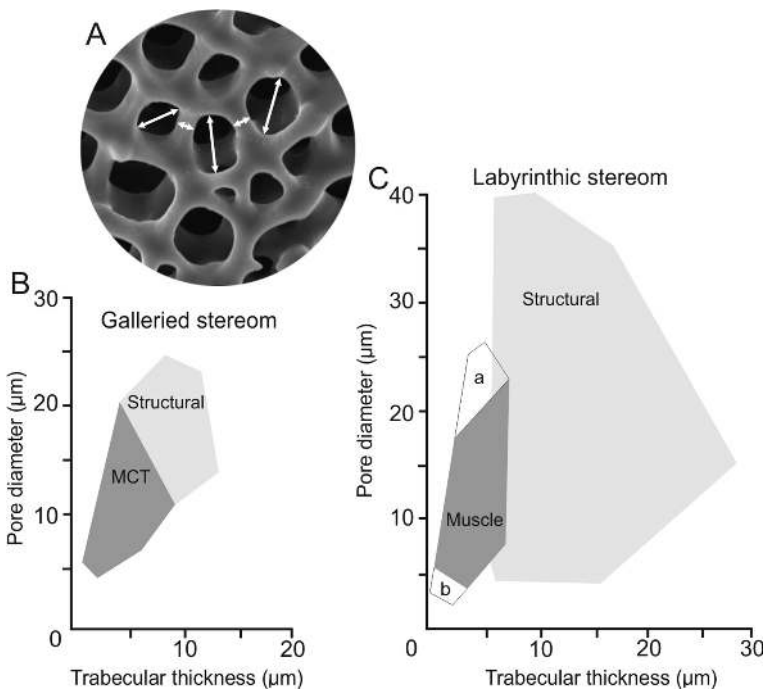

Figure 3 Quantification and functional importance of stereom. A. Example of measurements of pore diameter and trabecular thickness in stereom. B. Galleried stereom of all echinoderms for mutable collagenous tissues (MCT) and structural rectilinear stereom. C. Labyrinthic stereom of all echinoderms showing stereom associated with muscles, area "a" delimits stereom of deep-sea echinothurioid echinoid tubercle associated with collagenous insertion: area "b" delimits stereom associated with either muscle or collagenous fibers (B and C redrawn from Smith, 1990).

correlated with denser stereom microfabrics. Development of new labeling methods using stable isotope ^{26}Mg (Gorzelak et al., 2011; Gorzelak et al., 2014a) or trace element manganese (Gorzelak et al., 2017a) to study growth dynamics and morphogenesis of stereom at the micro- and sub-micrometer spatial resolution, confirmed and specified that the so-called open stereom may indeed grow very rapidly (>100 µm per day), but simultaneously it thickens at a very slow rate (~1 µm per day). Gorzelak et al. (2017a) also demonstrated that denser stereom microfabrics (perforate or labyrinthic constructional stereom) along the inner plate margins in echinoids form much more slowly than open rectilinear or galleried stereom expanding in interradial and meridional directions. The latter authors also showed that the

outermost perforate stereom in spines develops much more slowly than the inner rectilinear stereom. Likewise, formation of spine septa composed of imperforate stereom proceeds rather slowly and is a highly complex process involving deposition of porous stereom that is secondarily filled by calcite.

Notwithstanding, the nature of investing soft tissue is the most important factor controlling stereom design. Extensive studies on stereom microstructure of extant echinoderms (Roux, 1970, 1971, 1974, 1975, 1977; Heatfield, 1971; Macurda and Meyer, 1975; Macurda, 1976; Smith, 1980a) identified that each stereom type is commonly associated with a particular type of soft tissue. Smith (1990) pointed out that, by integrating quantitative and qualitative approaches, it is possible to distinguish areas of collagen, muscle fibers and epithelial tissue (Figure 3).

Collagenous fibers binding ossicles together are arranged in deeply penetrating and long straight bundles. As a consequence, stereom associated with this type of tissue typically appears in the form of well-aligned galleries (Grimmer el al., 1984). Muscles in echinoderm ossicles, in turn, usually splay out and are anchored around fine or moderately fine labyrinthic or retiform stereom, which forms a distinct platform growing peripherally. In crinoid arms, this stereom is typically associated with needle-like projections (Macurda and Meyer, 1975). However, if collagenous fibers are not penetrative and short, they may also loop around the trabeculae, superficially resembling labyrinthic stereom. For instance, at autotomy planes in crinoid columnals and brachials, collagenous fibers are short and thin, and anchor around labyrinthic-like stereom laying over galleried stereom (e.g., Gorzelak, 2018). Likewise, small and nonpenetrative collagenous fibers associated with pedicellariae and small spines attach to very fine labyrinthic stereom (trabecular thickness < ~4 μm; pore diameter < ~5 μm) (Smith, 1980a). Another exception is found in some deep-sea echinoids, such as echinothurioid echinoids in which collagenous fibers of their tubercles attach to open (pore diameter > ~17 μm) and fine (trabecular thickness ~2–8 μm) labyrinthic stereom (Figure 3), and in a few stalked crinoids (Hyocrinidae and Holopodidae) in which ligaments may also attach to labyrinthic stereom (Holland et al., 1991; Roux et al., 2002). These labyrinthic-like stereoms associated with short, non-penetrative collagenous fibers, in contrast to thin muscle-bearing labyrinthic or retiform stereom layer, are however usually extended to a thicker layer composed of at least a few levels and/or are more open textured (Smith, 1980a). The exception to this observation is the pillar bridges of echinoid teeth, which are composed of a retiform layer and bear collagenous ligaments. Noteworthy, although muscle fibers in spines of echinoids usually attach to superficial, open and irregularly arranged fine stereom, in certain species of cidaroids, spine muscles may be solely linked to unmodified rectilinear or galleried stereom (Smith, 1980a).

Stereom diagnostic for epithelial tissue is usually dense and thick. It appears in the form of coarse labyrinthic stereom or, most commonly, perforate to imperforate stereom layers. Superficially, these stereom types can be variously ornamented with pegs, domes or thorns. These stereom microfabrics display high stiffness and hardness, and are thought to increase skeletal strengthening and resistance to abrasion (e.g., Moureaux et al., 2010).

In the following, I have compiled data (Roux, 1970; Macurda and Meyer, 1975; Macurda, 1976; Smith, 1980a; 1990; Medeiros-Bergen, 1996; Reich, 2015; Martins and Tavares, 2018; Gorzelak, 2018) and provide a summary of each stereom type, with special references to their respective appearance, distribution and association with soft tissues.

3.1 Rectilinear Stereom

Regular array of trabeculae arranged in cubic (or orthorhombic) lattice. Pores well aligned and equal in three directions, perpendicular (or nearly perpendicular) to one another; their diameter is comparable to the thickness of the trabeculae (Figures 4A–D). It is commonly used for general plate construction (in echinoids and asteroids). It is also associated with penetrative collagenous tissues (in crinoid columnal and brachial articular faces).

3.2 Galleried Stereom

Deeply penetrating parallel galleries running in one direction only. No regular surface pattern. Lateral pores usually smaller than the galleried pores (Figures 4E–H). It is commonly associated with penetrative collagenous fibers (4–12 μm in diameter) running parallel to galleries (e.g., suture faces and boss of large tubercles in echinoids; suture faces in asteroid plates; brachial ligament pits, columnal, and cirral articular faces in crinoids; intervertebral and spine ligament insertion areas in ophiuroids). In some rare cases it may be connected with muscles inserting on outwardly growing surfaces (e.g., perradial muscle pits in asteroid plates).

3.3 Labyrinthic Stereom

Irregular meshwork of trabeculae. Trabeculae and pores form unorganized tangle at any section and may be of different size (Figures 4I–L):

(i) Fine meshwork (pores < ~6 μm, trabeculae < ~3 μm) is associated with attachment areas for fibrous tissues (commonly muscle, rarely collagenous) (e.g., small tubercle bosses and associated spine bases in echinoids, asteroids and ophiuroids; areoles of echinoid tubercles; muscle flanges of ophiuroid vertebrae; tube foot attachment areas in echinoids, asteroids and ophiuroids);

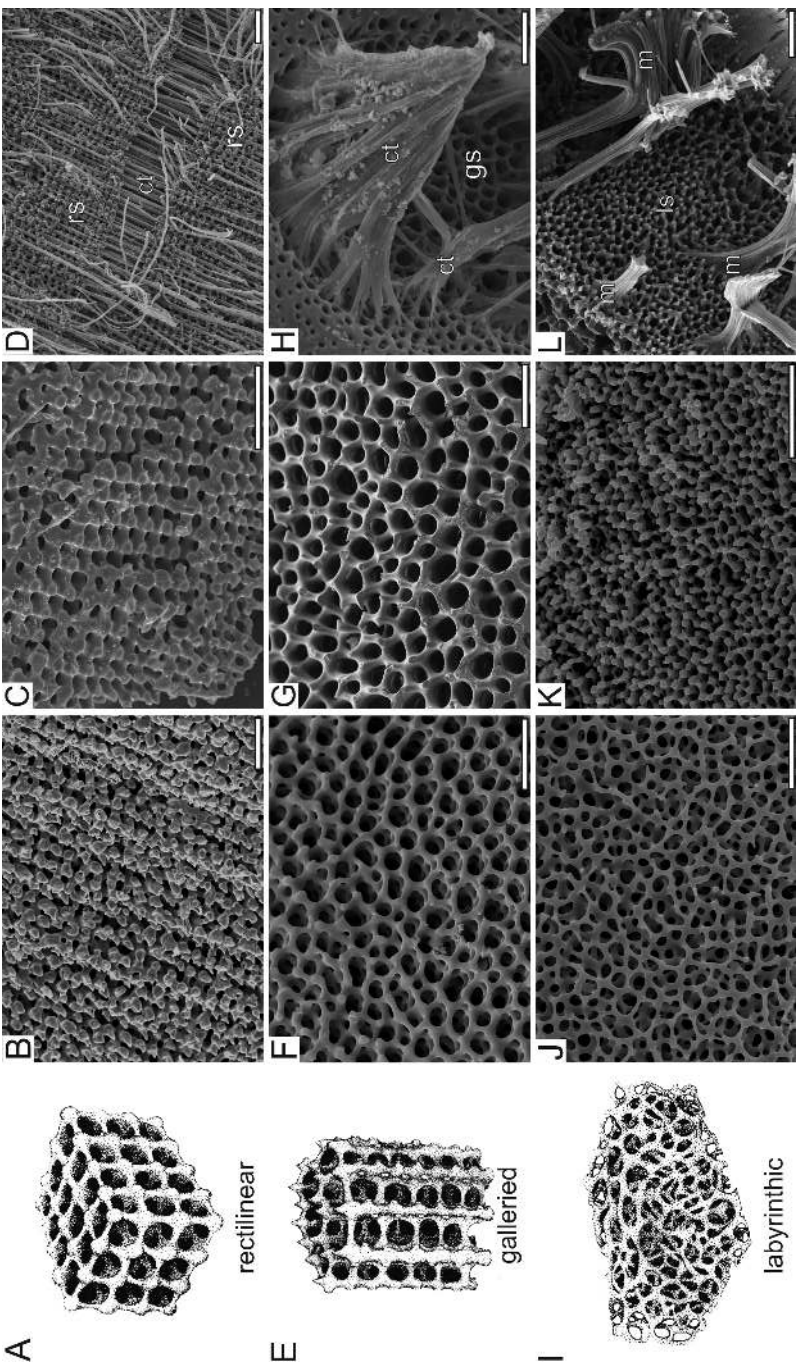

Caption for Figure 4 (cont.)

Figure 4 Different types of stereom fabrics in recent echinoderms. A–D. Rectilinear stereom: a schematic drawing (A, adopted from Smith, 1980a); ligament insertion area on a radial of a crinoid *Holopus rangi* Carpenter (B); penetrative collagenous tissue area on columnal facet of a crinoid *Metacrinus rotundus* Carpenter (C); long through-going collagenous ligamentary tissue (ct) penetrating rectilinear stereom (rs) in two columnals of *Metacrinus rotundus* Carpenter (D). E–H. Galleried stereom: a schematic drawing (E, adopted from Smith, 1980a); test plate of a cidaroid *Prionocidaris baculosa* Lamarck (collagenous sutural fiber area) (F); articular facets of a crinoid cirrus of *Metacrinus rotundus* Carpenter (ligament collagenous fibers [ct] penetrate galleried stereom [gs] (G, H)). I–L. Labyrinthic stereom: a schematic drawing (I, adapted from Smith, 1980a); muscle attachment area on demipiramids of an echinoid *Prionocidaris baculosa* Lamarck (J, K); muscle attachment areas (m) linked to labyrinthic stereom with needle-like projections on a brachial of crinoid *Metacrinus rotundus* Carpenter (L). Scale bars = 100 μm (A–D) and 50 μm (E–L), respectively.